

1 Liu Huaran, Lu Feiyu, Liu Zhengyu, Liu Yun, and Zhang Shaoqing, 2016: Assimilating
2 atmosphere reanalysis in coupled data assimilation. *J. Meteor. Res.*, **30**(4), doi:
3 10.1007/s13351-016-6014-1.(in press)
4
5
6

7 **Assimilating Atmosphere Reanalysis in Coupled** 8 **Data Assimilation**

9
10
11 LIU Huaran^{1,2} (刘华然), LU Feiyu² (卢飞雨), LIU Zhengyu² (刘征宇), LIU Yun³ (刘贇),
12 and ZHANG Shaoqing⁴ (张绍晴)

13
14
15
16 ¹ *Dept. Atmospheric Sciences, Nanjing University of Information Science & Technology, China*

17 ² *Dept. Atmospheric and Oceanic Sciences, University of Wisconsin-Madison, USA*

18 ³ *Dept. Atmospheric and Oceanic Science, University of Maryland, USA*

19 ⁴ *Geophysical Fluid Dynamics Laboratory, NOAA, Princeton, USA.*
20
21
22
23
24
25

26 (Received February 6, 2016; in final form May 5, 2016)
27
28

Supported by Nanjing University of Information Science and Technology

Corresponding author: Huaran Liu

Email: hliu287@wisc.edu.

©The Chinese Meteorological Society and Springer-Verlag Berlin Heidelberg 2016.

ABSTRACT

29
 30
 31 This paper tests the idea of substituting the atmospheric observations with atmospheric
 32 reanalysis when setting up a coupled data assimilation system. The paper focuses on the
 33 quantification of the effects on the oceanic analysis resulted from this substitution and
 34 designs four different assimilation schemes for such substitution . A coupled Lorenz96
 35 system is constructed and an ensemble Kalman filter is adopted. The atmospheric
 36 reanalysis and oceanic observations are assimilated into the system and the analysis
 37 quality is compared to a benchmark experiment where both atmospheric and oceanic
 38 observations are assimilated. Four schemes of assimilating the reanalysis are designed
 39 and they differ in the generation of the perturbed observation ensemble and the
 40 representation of the error covariance matrix. The results show that when the reanalysis is
 41 assimilated directly as independent observations, the RMSE increase of oceanic analysis
 42 relative to the benchmark is less than 16% in the perfect model framework; in the biased
 43 model case, the increase is less than 22%. This result is robust with sufficient ensemble
 44 size and reasonable atmospheric observation quality (e.g frequency, noisiness, density). If
 45 the observation is overly noisy, infrequent, sparse, or the ensemble size is insufficiently
 46 small, the analysis deterioration caused by the substitution is less severe since the
 47 analysis quality of the benchmark also deteriorates significantly due to worse
 48 observations and undersampling. The results from different assimilation schemes
 49 highlights the importance of two factors: accurate representations of the error covariance
 50 of the reanalysis and the temporal coherence along each ensemble member, which are
 51 crucial for the analysis quality of the substitution experiment.

52 **Key words:** data assimilation, reanalysis data, ensemble Kalman filter

53 1. Introduction

54
55 Coupled data assimilation (CDA) uses a coupled model to extract information from
56 observations that are available in one or more media and produces continuous time series
57 of the climate states. Compared to single component assimilation, CDA incorporates the
58 full impact of observations across the air-sea interface and allows the covariability of the
59 atmospheric and oceanic states, and thus it can provide consistent state estimation of the
60 coupled system for further study of the climate variability and the initialization of
61 coupled general circulation models (CGCM) (Kitoh and Arakawa, 1999; Arakawa and
62 Kitoh, 2004; Luo et al., 2008; Sugiura et al., 2008; Tardif et al., 2015; Zhang et al., 2005,
63 2007; Zhang, 2011). Despite the huge benefits and demand for CDA, the implementation
64 of CDA has both theoretical and technical challenges, for example, the estimation of the
65 coupled error covariance matrix (e.g. Lu et al., 2015; Han et al., 2013) and the huge
66 computational costs of CDA experiments in fully-coupled models. The NCEP Climate
67 Forecast System Reanalysis (CFSR) was completed for the period 1979-2009 (Saha et al.,
68 2010). It is a weak CDA system where the atmospheric and oceanic data assimilation are
69 performed independently and the coupling is only through model dynamics.

70 In this paper, we want to explore the idea of assimilating atmospheric reanalysis
71 data in a CDA system and its resultant consequences. This idea is motivated by the desire
72 to find an efficient way to get ocean analysis from a CDA process that incorporates both
73 the atmospheric and oceanic observations. The atmospheric observations include
74 hundreds of types with different formats, coverage, frequency, etc., which makes it nearly
75 impossible for an individual or a small group to collect and assimilate all these
76 observations to set up the CDA system independently. Reanalysis datasets incorporate

77 millions of observations, which includes, but is not limited to, radiosonde, satellite, buoy,
78 aircraft and ship reports, into a stable data assimilation system (e.g., [Kalnay et al., 1996](#);
79 [Kistler et al., 2001](#); [Kanamitsu et al., 2002](#); [Uppala et al., 2005](#); [Kobayashi et al., 2015](#);
80 [Saha et al., 2010](#); [Dee et al., 2011](#)). In addition, these datasets provide global coverage
81 with constant spatial and temporal resolution over three or more decades for hundreds of
82 variables (e.g., [Kalnay et al., 1996](#); [Kistler et al., 2001](#); [Kanamitsu et al., 2002](#); [Uppala et](#)
83 [al., 2005](#); [Kobayashi et al., 2015](#); [Saha et al., 2010](#); [Dee et al., 2011](#)), which makes
84 them relatively straightforward to handle from a processing standpoint. If it is feasible to
85 substitute the atmospheric reanalysis datasets for actual observational data, we can set up
86 CDA systems using different models much more easily and expect reasonable output of
87 model analysis, especially oceanic analysis. [Zhang et al.\(2007\)](#) has assimilated
88 atmospheric reanalysis directly as observations in a fully coupled climate model with a
89 CDA system, without the examination of the possible effects brought out by the
90 substitution. Yet their results are still promising and their assimilation successfully
91 reconstructs the twentieth-century ocean heat content variability and trends in most
92 locations. This indicates that it is feasible to substitute the atmospheric observations with
93 reanalysis in a CDA process. However, the resultant effects on the analysis from the
94 substitution is never carefully studied. In this paper, we will test this idea with an
95 emphasis on the quantification of the resultant effects from the substitution, and
96 investigates the assimilation schemes associated with this substitution.

97 A coupled Lorenz96 model ([Lorenz, 1996](#)) representing the atmosphere and the ocean
98 is constructed to test the idea of assimilating atmospheric reanalysis data as observations
99 in a CDA system. The results will be compared to the best-case scenario (benchmark)

100 where both the atmospheric and oceanic observations are assimilated. The paper is
 101 organized as follows: the methodology is shown in section 2; experiments and results are
 102 presented in section 3; tests on different assimilation schemes are shown in section 4;
 103 section 5 provides a concluding summary.

104 **2. Methodology**

105 *2.1 The model*

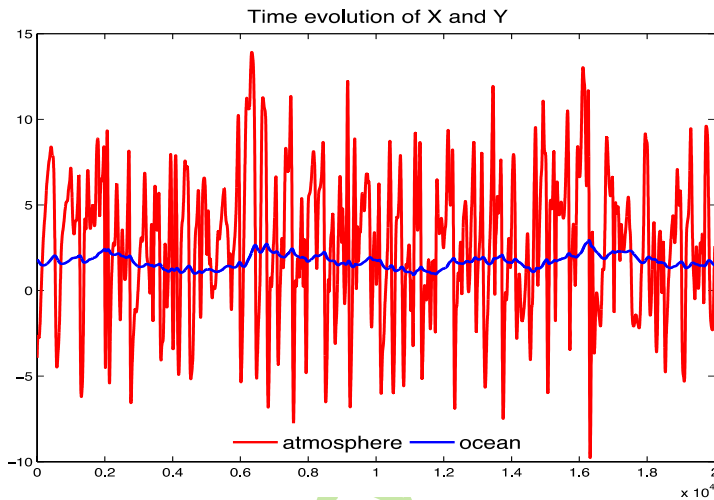
106
 107 A dynamical system is set up by coupling two 40-variable ($n_v=40$) Lorenz96 systems
 108 (Lorenz, 1996), one representing the atmosphere (Eq.1) and the other representing the
 109 ocean (Eq.2).

$$\begin{aligned}
 110 \quad & \frac{dX_j}{dt} = \\
 111 \quad & [X_{j+1} - X_{j-2}] * X_{j-1} - (1 - C_a) * X_j + F_a + C_a * \\
 112 \quad & [Y_j - \\
 113 \quad & X_j]. \tag{1}
 \end{aligned}$$

$$\begin{aligned}
 115 \quad & M * \frac{dY_j}{dt} = \\
 116 \quad & [Y_{j+1} - Y_{j-2}] * Y_{j-1} - Y_j + F_o + C_o * \\
 117 \quad & [X_j - \\
 118 \quad & Y_j]. \tag{2}
 \end{aligned}$$

119 The atmosphere and ocean are coupled through the flux terms $C_a * [Y_j - X_j]$ and
 120 $C_o * [X_j - Y_j]$, where $C_a = 2.0$ and $C_o = 0.1$ are the coupling coefficients for the
 121 atmosphere and ocean, respectively. F_a and F_o represent the external forcing, and in this
 122 case $F_a = 8$, $F_o = 0$ such that the ocean is only forced by the atmosphere. The oceanic

123 timescale is controlled by coefficient M , which is chosen to be 20. Fig.1 shows the typical
 124 time evolution of variables X_1 and Y_1 . The climatological standard deviations averaged
 125 over 40 variables for X and Y are 3.86 and 0.47, respectively. Therefore, the
 126 observational errors are arbitrarily set at 1.0 for the atmosphere and 0.1 for the ocean. In
 127 all experiments, the integration time step is 0.005, and 1 time unit is roughly 5 days. We
 128 forward the model for $2 * 10^5$ time steps (1000 time units). The first 20000 spin-up steps
 129 are discarded when we evaluate the analysis quality.



130
 131 **Fig. 1.** Typical time evolution of X_1 (red) and Y_1 (blue).

132
 133 *2.2 The assimilation procedure and diagnostics*

134 We will employ the ensemble Kalman filter (EnKF) with perturbed observation (Evensen,
 135 1994; Burgers et al., 1998; Houtekamer and Mitchell, 1998). 80 ensemble members are
 136 used ($ens = 80$). Covariance localization is performed by applying a Schur product
 137 (Schur, 1911) to the forecast error covariance matrix (Gaspari and Cohn, 1999).
 138 Covariance inflation is also applied with the relaxation method by Zhang et al. (2004).
 139

140 The root-mean-square error (RMSE) from all analysis steps is calculated to evaluate the
 141 data assimilation performance, given by

$$142 \quad \text{RMSE} = \sqrt{\frac{1}{nt} \frac{1}{nv} \sum_t \sum_i [X_{i,t} - X_{i,t}^T]^2} . \quad (3)$$

143 Where X_i and X_i^T are analysis and truth, respectively, at gridpoint i and time step t . In
 144 reality, the benchmark experiment would be the best-case scenario for a CDA system and
 145 should produce the best analysis possible. Therefore, it is used to evaluate the
 146 performance of our proposed schemes. The RMSE of different experiments that
 147 assimilate the reanalysis are then normalized by that of the benchmark experiment as in
 148 Eq.4

$$149 \quad \text{Ratio} = \frac{R - R_b}{R_b} \times 100\% . \quad (4)$$

150 where R represents the RMSE of the experiment in which the atmospheric reanalysis is
 151 assimilated as observation, and R_b represents the RMSE of the benchmark experiment.
 152 We repeat 90 simulations for each experiment and the results are displayed via boxplots.

153 *2.3 Model framework*

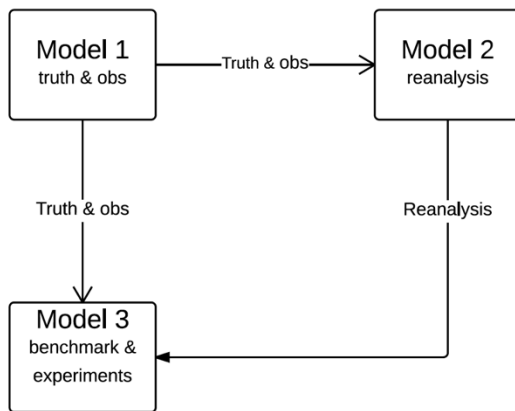
154
 155 In this section, we will introduce 3 models that are used to generate the true state,
 156 reanalysis and conduct the experiments respectively. The purpose of this is to allow for
 157 model bias to test the robustness of the quantified effects. If these three models are the
 158 same, then it is a perfect model framework with no model bias.

159 Model 1: Generate the true state and observation. The true state is a control run of
 160 this model and the observations are generated by adding a Gaussian white noise $N(0, \sigma_o)$
 161 to the true state, where σ_o is the observational error.

162 Model 2: Generate reanalysis by assimilating observations from model 1. This
 163 mimic the fact that different research centers generate the reanalysis through their own
 164 GCMs (e.g. Kalnay et al., 1996; Kistler et al., 2001; Uppala et al., 2005; Kobayashi et al.,
 165 2015; Saha et al., 2010) and these GCMs are biased with regard to the the model used to
 166 generate the true state.

167 Model 3: Conduct the benchmark and substitution experiments. Model 3 is
 168 different from model 2 in that the model where CDA system is set up can be different
 169 from the model used to generate reanalysis.

170 The relationship among the three models is illustrated in Fig.2. In the perfect
 171 model framework, three models are the same and they use the default parameter values
 172 with Runge-Kutta 4 (RK4) integration scheme; In the biased mode framework, model
 173 bias is mimicked by different integration schemes and slight variations on model
 174 parameters. The detailed setup is summarized in Table.1.



175
 176 **Fig. 2.** Illustration of model setup. Truth and observations are generated in model 1.
 177 Reanalysis is generated in model 2. Experiments are conducted in model 3. In perfect
 178 model case the three models are the same, while in biased model case all three are
 179 different from each other.

180
181
182
183

	Integration Scheme	Model Parameters
Model 1	Runge-Kutta 2	Standard parameters
Model 2	Runge-Kutta 2	5% increase from Standard parameters
Model 3	Runge-Kutta 4	Standard parameters

184 **Table 1.** Model setup in biased model framework

185

186 **2.4 The benchmark and substitution experiment**

187 In the benchmark experiment conducted in model 3, atmospheric and oceanic
188 observations generated in model 1 are assimilated. Variables $X_1, X_3, X_5, \dots, X_{39}$ are
189 observed every 20 integration time steps and variables $Y_1, Y_3, Y_5, \dots, Y_{39}$ are observed
190 every 40 integration time steps, unless specified otherwise. This is the best-case scenario
191 where all observations that are available are assimilated.

192 The atmospheric reanalysis data used for the substitution experiments is generated
193 in model 2. The observations are the same as that in the benchmark experiment except no
194 oceanic observations are assimilated since the effects of the ocean data assimilation on
195 the atmosphere are small in this coupled Lorenz96 system. The reanalysis is the ensemble
196 mean output. We also preserve the reanalysis ensemble for the assimilation scheme
197 design later.

198 In the substitution experiments, the atmospheric reanalysis and oceanic
 199 observations are assimilated into model 3. The reanalysis is assimilated with the same
 200 frequency as the benchmark experiment, while oceanic observations stay unchanged.
 201 Although the atmospheric observations are not available at every gridpoint, the reanalysis
 202 will provide additional observations at unobserved locations..

203 *2.5 Assimilating the reanalysis*

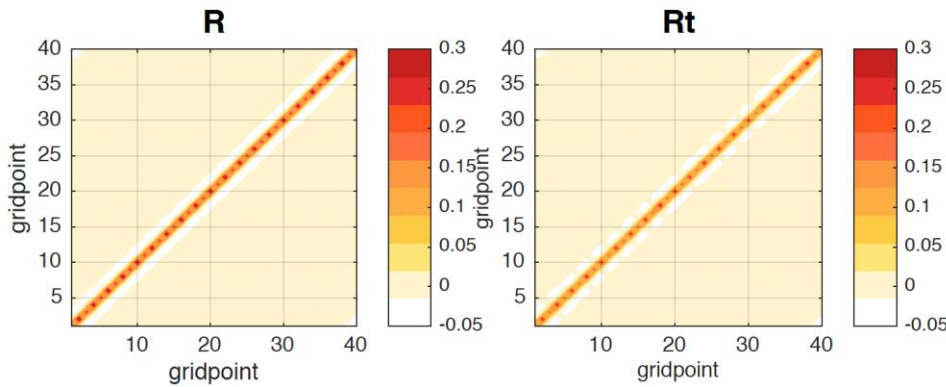
204
 205 The most straightforward way to assimilate the reanalysis is to simply treat the reanalysis
 206 as independent observations. First the error covariance matrix of the reanalysis is
 207 calculated, and then the reanalysis is independently perturbed according to the diagonal
 208 values of the matrix, namely the variances of the observations. The error covariance
 209 matrix of the reanalysis can be calculated as below:

210
$$R_t = cov < X - X^T > \quad (5)$$

$$= \begin{bmatrix} cov < X_1 - X_1^T, X_1 - X_1^T > & cov < X_1 - X_1^T, X_2 - X_2^T > & \dots & cov < X_1 - X_1^T, X_{40} - X_{40}^T > \\ cov < X_2 - X_2^T, X_1 - X_1^T > & cov < X_2 - X_2^T, X_2 - X_2^T > & \dots & cov < X_2 - X_2^T, X_{40} - X_{40}^T > \\ \vdots & \vdots & \ddots & \vdots \\ cov < X_{40} - X_{40}^T, X_1 - X_1^T > & cov < X_{40} - X_{40}^T, X_2 - X_2^T > & \dots & cov < X_{40} - X_{40}^T, X_{40} - X_{40}^T > \end{bmatrix}$$

211
 212 where X and X^T are the time series of the reanalysis and truth respectively; $cov <>$
 213 calculates the covariance. R_t is shown in Fig.3. The reanalysis at any given location is
 214 perturbed with Gaussian noise that has the same standard deviation as the square root of
 215 the corresponding diagonal element in R_t . Consequently, the error matrix used in
 216 calculating the Kalman gain is the R_t matrix with its off-diagonal elements set to zero due
 217 to the assumption of independence among different observations. In the real world,
 218 however, X^T is unknown. We can either use observation to replace X^T in Eq.5, or we can

219 use the averaged sample covariance of the original reanalysis ensemble (see R in Eq.7),
 220 which will be introduced later in section 4.

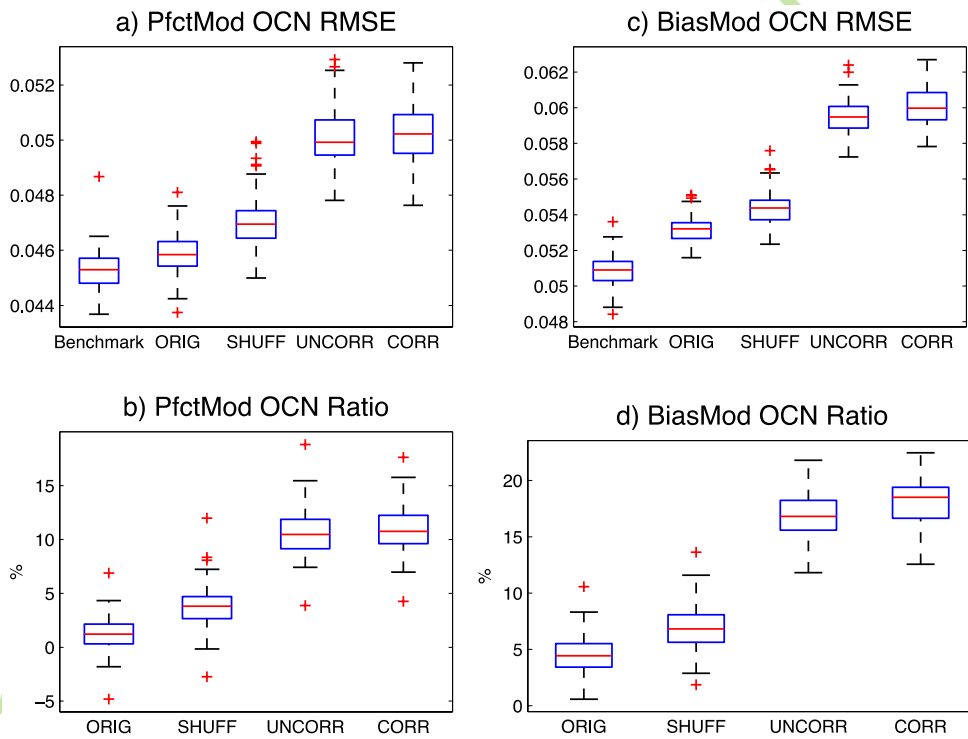


221
 222 **Fig. 3.** (left) The time average of flow-independent ensemble covariance matrix R and
 223 (right) the temporal covariance matrix R_t . Point (i, j) indicates the covariance between the
 224 i^{th} and j^{th} atmospheric variables.

225
 226 **3. Experiments and results**

227 Following the procedure in section 2d, the first type of experiment is denoted as
 228 UNCORR in Fig.4, which stands for “uncorrelated observation ensemble” since the
 229 observation ensemble is the reanalysis plus independent Gaussian white noise. Compared
 230 to the benchmark, the increase of the average RMSE of the ocean variables over 90
 231 simulations is 11.41% in the perfect model framework and 16.93% in the biased model
 232 framework. For the 90 simulations in the perfect model framework (Fig. 4b), the
 233 maximum and minimum RMSE increase are 15.46% and 7.42%. In the biased model
 234 framework (Fig. 4d), the maximum and minimum non-outlier RMSE increase are 21.79%
 235 and 11.81%. If only ocean data assimilation is carried out in this coupled Lorenz96 model,
 236 the ocean component will not be constrained by the oceanic observations alone and the
 237

238 oceanic RMSE can reach the climatological standard deviation. This is because in this
 239 simple coupled model, the ocean component is purely driven by the atmosphere and the
 240 feedback from the ocean to the atmosphere is small, hence we are not able get a
 241 reasonable oceanic analysis if the atmosphere is not well constrained. In this sense,
 242 substituting the atmospheric observations with the atmospheric reanalysis in a CDA
 243 process is better than assimilating oceanic observations alone in a coupled system. The
 244 performance of assimilating reanalysis is further tested with varied atmospheric
 245 observation frequency, atmospheric observation error, atmospheric observation density
 246 and ensemble size.



247

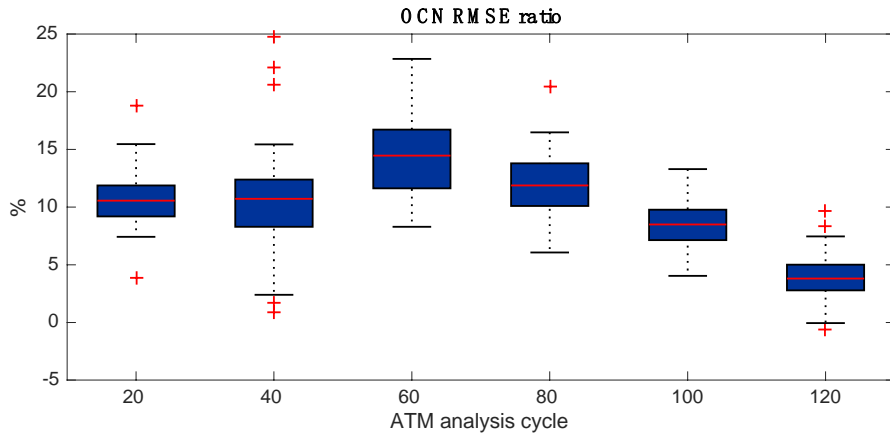
248

249 **Fig. 4.** Boxplots of 90 simulations for benchmark and the 4 different schemes named
 250 ORIG, SHUFF, UNCORR, and CORR. The left panel is the perfect model case and the
 251 right panel is the biased model case. The top panel shows the RMSE while the bottom

252 panel shows the RMSE ratio which is normalized by the benchmark experiment. The
253 whiskers below and above the box show minimum and maximum value. The upper and
254 lower bounds of the box are the first and third quartiles. The red line is the median and
255 the red crosses indicate the outliers.

256

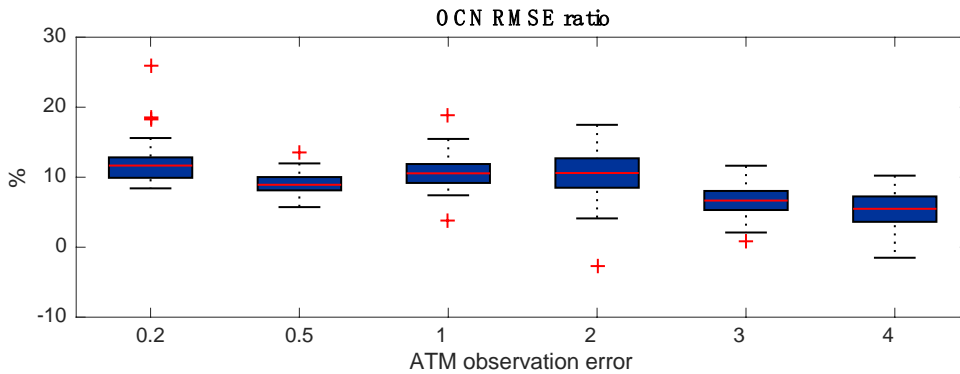
257 The performance of UNCORR is tested for different atmospheric observation
258 frequencies and the results are shown in Fig. 5. The analysis cycle increases from 20 to
259 120 as the atmosphere observations becomes infrequent. the RMSE of both UNCORR
260 and the benchmark increase due to decreased observational information (Figure not
261 shown). The ratios in Fig.5 show no significant trend when the analysis cycle increases
262 from 20 steps to 80 steps. However, as the atmospheric observation frequency becomes
263 unrealistically infrequent (every 80 steps and beyond, this frequency is like less than 1
264 observation every 2 days), the ratios tend to decrease. This means that as the analysis
265 quality get worse for both the benchmark and the substitution experiment due to less
266 available observational information, the difference between the benchmark and the
267 substitution experiment is smaller. That is to say, the resultant analysis deterioration from
268 the substitution is less severe.



270 **Fig. 5.** Sensitivity of ocean RMSE (top) and RMSE ratio (bottom) to atmosphere
 271 observation frequency for the UNCORR scheme over 90 simulations.

272

273 The sensitivity of UNCORR to varied atmospheric observation error is shown in
 274 Fig. 6. The absolute RMSE of both UNCORR and benchmark increase as the
 275 observations become more and more noisier (Figure not shown), while the ratios in Fig. 6
 276 show small fluctuations when the atmospheric observation error increases from 0.2 to 2.0,
 277 and eventually decrease as the error gets unrealistically large (beyond 2.0, more than half
 278 of the climatological standard deviation). This indicates that the oceanic analysis
 279 deterioration in UNCORR is fairly insensitive to the atmospheric observation error when
 280 it is in a reasonable range; In addition, the deterioration is lessened if the oceanic analyses
 281 of both the benchmark and the substitution experiment get worse due to the overly noisy
 282 observations.

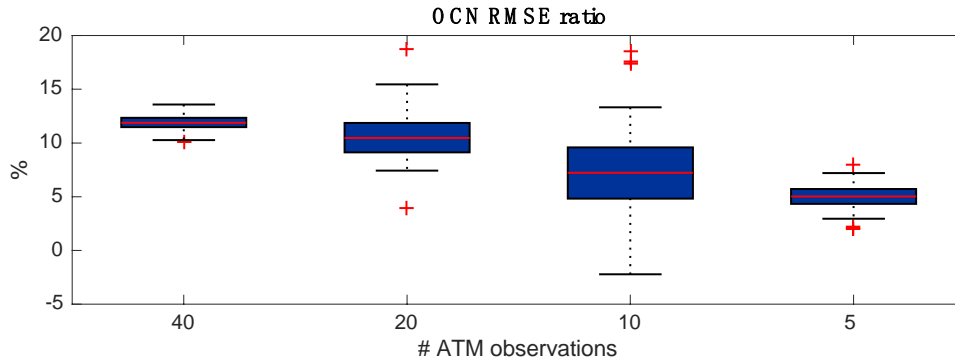


2...

284 **Fig. 6.** Same as Fig.5, but for different atmospheric observation errors.

285

286 The results of experiments with varied observation density but still evenly distributed
 287 observations are shown in Fig.7. The RMSE for both experiments are larger with sparser
 288 observations and smaller with denser observation (Figure not shown). The ratios in Fig. 7
 289 shows a consistent decreasing trend as the observations get denser. This suggests that the
 290 difference between the substitution and benchmark experiments is less significant if the
 291 analyses of both experiments get worse due to less observations, which is similar to the
 292 previous sensitivity tests. In contrast, if every variable is observed, the increase of RMSE
 293 in the substitution experiment relative to the benchmark is the most significant. In reality,
 294 the number of atmospheric observations is more or less fixed, and the density change will
 295 not be as extreme as in this simple sensitivity test. It is notable that as the observations
 296 get intermediately sparse, the data assimilation process gets less stable: the variance of
 297 ratios among the 90 simulations is noticeably bigger when there are only 10 or 20
 298 observations. This can be explained by the numerical instabilities developed in a sparse
 299 observation network with finite ensemble size (Gottwald and Majda, 2013).



3

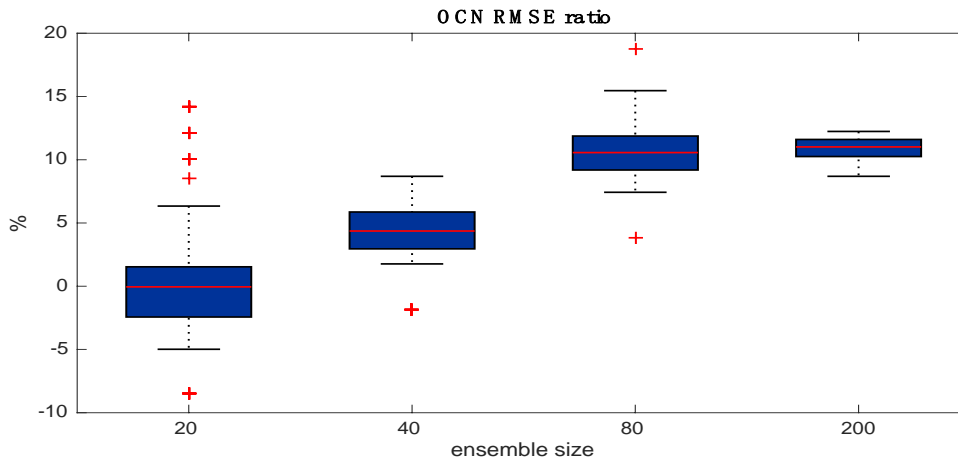
301 **Fig. 7.** Same as Fig.5, but for different observation densities.

302

303 The results in Figs. 5, 6 and 7 collectively indicate that the decrease in analysis
 304 quality due to the substitution is insensitive to the observation quality (frequency,
 305 noisiness, density) within a reasonable range. Meanwhile, when the quality of
 306 observation declines too much, the decrease in analysis quality caused by substitution
 307 becomes less severe compared to the benchmark because the analysis quality of the
 308 benchmark also decreases significantly due to poor observational quality.

309 Ensemble size is an important factor in the estimation of error covariance and
 310 correlation. Additional experiments with ensemble size 20, 40, and 200 are shown in
 311 Fig.8. The RMSEs of both experiments decrease with increasing ensemble size (Figure
 312 not shown). The ratios in Fig.8 increases with ensemble size and eventually levels off.

313 This suggests that with smaller sample size, the bad analysis quality for both experiments
 314 will lead to smaller RMSE contrast between the substitution and the benchmark
 315 experiments, thus smaller ratios. Vice versa for sufficiently large sample size.



316

317 **Fig. 8.** Same as Fig.5, but for different ensemble sizes.

318

319 **4. Tests on assimilating schemes**

320

321 In the last section, the UNCORR experiments assume that the analysis has independent
 322 errors at different locations, which, however, is not the case in reality. When reanalysis is
 323 generated, different model locations are connected through both model dynamics and the
 324 use of localization schemes. Thus the analysis errors will be spatially correlated between
 325 nearby or even far-apart locations. In addition, the analysis errors can also persist through
 326 time, hence there is also temporal correlation in the time series of the analysis. The
 327 previous UNCORR experiment neglects both the spatial and temporal correlations, which
 328 may affect the performance of the CDA scheme. To deal with these correlations and
 329 investigate how they affect the CDA, we tested three other schemes of treating the
 330 reanalysis error covariance, which are named as CORR, ORIG, and SHUFF.

331

332

First in the CORR scheme, the off-diagonal correlation among different variables
 of the reanalysis is taken into consideration. Instead of being set to zero as in UNCORR,

333 the off-diagonal elements in the reanalysis error covariance matrix R_t are retained. In
 334 correspondence, a spatially correlated observation ensemble is attained by perturbing the
 335 reanalysis with correlated noise. The spatial correlation among different variables can be
 336 calculated in a similar way as R_t in Eq.5: $C = corr \langle X - X^T \rangle$.

337 (6)

338 The average RMSE increase of ocean variables over 90 simulations in CORR is 11.79%
 339 for the perfect model framework and 18.13% for the biased model framework. The
 340 maximum and minimum non-outlier RMSE increase are 15.76% and 6.96% for 90
 341 simulations in the perfect model framework (Fig.4a) and are 22.45% and 12.55% in
 342 biased model framework (Fig.4b). Although CORR includes the off-diagonal correlation
 343 among different variables, it does not outperform UNCORR and is also less stable. This
 344 is mainly caused by the additional sampling errors. Because of the chaotic nature of the
 345 model, the correlation among different locations in Lorenz96 decreases below 0.2 within
 346 five gridpoints. Thus CORR is subject to significant sampling error in two processes,
 347 firstly when the correlation matrix is calculated in Eq.6 and secondly when the correlated
 348 observation ensemble is artificially generated based on the correlation matrix. With a
 349 finite sample size, the error in the covariance or correlation estimates greatly increases
 350 when the true correlation becomes smaller. Therefore, although including the spatial
 351 correlation may improve the performance theoretically, the additional sampling error
 352 overwhelms the possible improvement.

353 The second ORIG scheme uses the original reanalysis ensemble as the “perturbed”
 354 observation ensemble during CDA. The original reanalysis ensemble is the byproduct of
 355 the ensemble-based DA filter during the generation of the reanalysis, therefore they could

356 accurately capture not only the flow-dependent correlation information among different
 357 locations, but also the temporal coherence of each ensemble member at every location.
 358 The error covariance matrix in this scheme is calculated as the time average of the error
 359 covariance matrix of the reanalysis ensemble over each analysis step.

$$360 \quad R = \text{mean} \langle \text{cov} \langle X_t^{re}(nv, ens) \rangle \rangle. \quad (7)$$

361 where $\text{cov} \langle \cdot \rangle$ and $\text{mean} \langle \cdot \rangle$ represents sample covariance and average over time
 362 respectively. X_t^{re} represents the original reanalysis ensemble at analysis time step t . R is
 363 quantitatively similar to Rt and is also diagonally dominant (Fig.3). The performance of
 364 ORIG is noticeably better than UNCORR and CORR (Fig.4) and is fairly close to the
 365 benchmark. The average oceanic RMSE increase over 90 simulations is 2.02% in the
 366 perfect model framework and 4.64% in the biased model framework. The ratio ranges
 367 from -1.81% to 4.33% in the perfect model framework over 90 simulations (Fig. 4a), and
 368 from 0.58% to 8.31% in the biased model framework.

369 The third SHUFF scheme is used to test the relative importance of accurate spatial
 370 correlation and temporal coherence in the improvement from CORR to ORIG. SHUFF is
 371 the same as ORIG except that the original reanalysis ensemble is shuffled at each analysis
 372 step before it is assimilated, hence the temporal coherence carried along each ensemble
 373 member is removed in SHUFF while the off-diagonal spatial correlation is still preserved.
 374 The performance of SHUFF is slightly worse than ORIG in both perfect and biased
 375 model case (Fig.4), which indicates that the temporal coherence of the reanalysis
 376 ensemble is less important for the ocean analysis. Meanwhile, SHUFF, similar to ORIG,
 377 outperforms UNCORR and CORR significantly: the highest RMSE increase in SHUFF
 378 (7.22%) almost approaches the lowest one in CORR (6.96%) and UNCORR (7.42%).

379 Recall that SHUFF and CORR both have the off-diagonal correlation and do not have the
 380 temporal coherence, and they primarily differ in generating the perturbations for the
 381 reanalysis (Eq.5 and Eq.7), or simply the magnitude of sampling errors for the correlation
 382 matrix. The comparisons between SHUFF and CORR and between SHUFF and ORIG
 383 therefore suggest that accurate representation of the spatial correlation is relatively more
 384 important than the temporal coherence for the ocean analysis. However, for the
 385 atmosphere component, the performance of SHUFF is closer to CORR than to ORIG
 386 (figure not shown), which suggests a relatively more important role of temporal
 387 coherence for the atmospheric analysis. All the assimilation schemes tested are
 388 summarized in Table 2.

389

	Covariance Matrix	Observation Ensemble
ORIG	Eq.7	Original reanalysis ensemble
SHUFF	Eq.7	Shuffled original reanalysis ensemble
UNCORR	Eq.5, off-diagonal elements set to zero	Perturbed ensemble (uncorrelated)
CORR	Eq.5	Perturbed ensemble based on correlation matrix

390 **Table 2.** Assimilation scheme design

391 **5. Summary and conclusions**

392

393 We substituted the atmospheric observations with reanalysis data to set up a CDA system
 394 in coupled Lorenz96 models and quantified the resultant effects on the oceanic analysis.

395 We compared the the oceanic RMSE of the substitution experiment where atmospheric
 396 reanalysis and oceanic observations are assimilated, to a benchmark experiment where

397 both atmospheric and oceanic observations are assimilated. It is found that the
398 substitution results in the deterioration of oceanic analysis quality. The magnitude of this
399 deterioration depends on how the reanalysis is assimilated. When the reanalysis is
400 assimilated directly as independent observations (UNCORR) as in Zhang et al. 2007, , the
401 oceanic RMSE increase due to the substitution is about 16% in perfect model framework
402 and about 22% in the biased model framework compared to the benchmark, or best-case
403 scenario. Additional sensitivity tests show that this result is robust with sufficient
404 ensemble size and reasonable atmospheric observation quality (density, frequency,
405 noisiness). If the ensemble size is smaller, or the observation quality is worse (less
406 frequent, sparser, noisier), the deterioration will become less severe because the analysis
407 quality of the benchmark also decreases significantly.

408 In addition to the direct method, three supplementary schemes (CORR, ORIG,
409 SHUFF) are tested with a focus on the representation of the background error covariance
410 matrix and the generation of the perturbed observations in EnKF. We found that both the
411 spatial correlation among the reanalysis data points and the coherence along each original
412 reanalysis ensemble member are crucial to the analysis quality of the substitution
413 experiments: The oceanic RMSE increase is significantly reduced when the temporal
414 coherence along each member of the original reanalysis ensemble is preserved (ORIG);
415 the removal of such ensemble member coherence (SHUFF, CORR) and inaccurate
416 capture of the off-diagonal correlation (CORR, UNCORR) will result in the increase of
417 RMSE . However, the relative importance between the off-diagonal correlation and
418 temporal coherence on analysis quality is different for the atmosphere and ocean
419 component. For the ocean component, the RMSE of SHUFF is closer to ORIG than

420 CORR, indicating a relative more important influence from the accurate representation of
421 spatial correlation than temporal coherence, while for the atmosphere, it is the other way
422 round.

423 This study has demonstrated that substituting the atmospheric observations with
424 atmospheric reanalysis is a potentially efficient approach to implement CDA systems at
425 the cost of moderate degradation of analysis quality. Despite the fact that this degradation
426 can not be eliminated, the CDA products can still provide state-estimation of the coupled
427 variability in the atmosphere-ocean system which incorporates both the observational and
428 model information, and the dynamical balance between the atmosphere and ocean
429 components can reduce the initial shock in the initialization of coupled GCM. There are
430 still remaining issues regarding assimilating atmospheric reanalysis data. First, different
431 schemes, in particular ORIG, UNCORR and CORR, should be tested on models that have
432 higher spatial correlations and the impact on the oceanic analysis quality should be
433 evaluated. Second, different ensemble filters such as ensemble adjustment filter ([Zhang et](#)
434 [al., 2007](#); [Anderson, 2001](#)), can be employed to assess robustness of the assimilating the
435 reanalysis. Finally, this idea should be further tested in a coupled model of higher
436 complexity.

437
438 ***Acknowledgment:***

439
440 We gratefully thank Shan Li for helpful discussions. This research is sponsored by
441 Nanjing University of Information Science and Technology.

442

443 **References**

- 444 Anderson, J. L., 2001: An ensemble adjustment Kalman filter for data assimilation. *Mon. Wea. Rev.*,
445 **129**, 2884–2903, doi: 10.1175/1520-0493(2001)129<2884:AEAKFF>2.0.CO;2.
- 446 Arakawa, O., and A. Kitoh, 2004: Comparison of local precipitation–SST relationship between the
447 observation and a reanalysis dataset. *Geophys. Res. Lett.*, **31**, L12206, doi: 10.1029/2004GL020283.
- 448 Burgers, G., P. J. van Leeuwen, and G. Evensen, 1998: Analysis scheme in the ensemble Kalman
449 filter. *Mon. Wea. Rev.*, **126**, 1719–1724, doi: 10.1175/1520-0493(1998)126<1719:ASITEK>2.0.CO;2.
- 450 Chen, D., S. E. Zebiak, A. J. Busalacchi, et al., 1995: An improved procedure for El Niño forecasting:
451 implications for predictability. *Science*, **269**, 1699–1702, doi: 10.1126/science.269.5231.1699.
- 452 Dee, D. P., S. M. Uppala, A. J. Simmons, et al., 2011: The ERA-Interim reanalysis: configuration and
453 performance of the data assimilation system. *Quart. J. Roy. Meteor. Soc.*, **137**, 553–597, doi:
454 10.1002/qj.828.
- 455 Evensen, G., 1994: Sequential data assimilation with a nonlinear quasi-geostrophic model using
456 Monte Carlo methods to forecast error statistics. *J. Geophys. Res.*, **99**, 10143–10162, doi:
457 10.1029/94JC00572.
- 458 Fujii, Y., T. Nakaegawa, S. Matsumoto, et al., 2009: Coupled climate simulation by constraining
459 ocean fields in a coupled model with ocean data. *J. Clim.*, **22**, 5541–5557, doi:
460 10.1175/2009JCLI2814.1.
- 461 Gaspari, G., and S. E. Cohn, 1999: Construction of correlation functions in two and three dimensions.
462 *Quart. J. Roy. Meteor. Soc.*, **125**, 723–757, doi: 10.1002/qj.49712555417.
- 463 Gottwald, G. A., and A. J. Majda, 2013: A mechanism for catastrophic filter divergence in data
464 assimilation for sparse observation networks. *Nonlinear Process. Geophys.*, **20**, 705–712, doi:
465 10.5194/npg-20-705-2013.
- 466 Hamill, T. M., J. S. Whitaker, and C. Snyder, 2001: Distance-dependent filtering of background error
467 covariance estimates in an ensemble Kalman filter. *Mon. Wea. Rev.*, **129**, 2776–2790, doi:
468 10.1175/1520-0493(2001)129<2776:DDFOBE>2.0.CO;2.

- 469 Han, G. J., X. R. Wu, S. Q. Zhang, et al., 2013: Error covariance estimation for coupled data
 470 assimilation using a Lorenz atmosphere and a simple pycnocline ocean model. *J. Clim.*, **26**, 10218–
 471 10231, doi: 10.1175/JCLI-D-13-00236.1.
- 472 Houtekamer, P. L., and H. L. Mitchell, 1998: Data assimilation using an ensemble Kalman filter
 473 technique. *Mon. Wea. Rev.*, **126**, 796–811.
- 474 Kalnay, E., M. Kanamitsu, R. Kistler, et al., 1996: The NCEP/NCAR 40-Year Reanalysis Project. *Bull.*
 475 *Amer. Meteor. Soc.*, **77**, 437–472. doi: 10.1175/1520-0477(1996)077<0437:TNYRP>2.0.CO;2.
- 476 Kanamitsu, M., W. Ebisuzaki, J. Woollen, et al., 2002: NCEP–DOE AMIP-II reanalysis (R-2). *Bull.*
 477 *Am. Meteor. Soc.*, **83**, 1631–1643, doi: 10.1175/BAMS-83-11-1631.
- 478 Kistler, R., W. Collins, S. Saha, et al., 2001: The NCEP-NCAR 50 -year reanalysis: monthly means
 479 CD-ROM and documentation. *Bull. Am. Meteor. Soc.*, **82**, 247–267, doi: 10.1175/1520-
 480 0477(2001)082<0247:TNNYRM>2.3.CO;2.
- 481 Kitoh, A., and O. Arakawa, 1999: On overestimation of tropical precipitation by an atmospheric GCM
 482 with prescribed SST. *Geophys. Res. Lett.*, **26**, 2965–2968, doi: 10.1029/1999GL900616.
- 483 Kobayashi, S., Y. Ota, Y. Harada, et al., 2015: The JRA- 55 reanalysis: general specifications and
 484 basic characteristics. *J. Meteor. Soc. Japan*, **93**, 5–48, doi: 10.2151/jmsj.2015-001.
- 485 Liu, Z. Y., S. Wu, S. Q. Zhang, et al., 2013: Ensemble data assimilation in a simple coupled climate
 486 model: the role of ocean-atmosphere interaction. *Adv. Atmos. Sci.*, **30**, 1235–1248, doi:
 487 10.1007/s00376-013-2268-z.
- 488 Lorenz, E. N., 1996: Predictability—A Problem Partly Solved. *Proceedings of Seminar on*
 489 *Predictability, I, ECMWF, Reading, Berkshire, UK*, 1–18.
- 490 Lu, F. Y., Z. Y. Liu, S. Q. Zhang, et al., 2015: Strongly coupled data assimilation using leading
 491 averaged coupled covariance (LACC). Part II: CGCM Experiments. *Mon. Wea. Rev.*, **143**, 4645–4659.
- 492 Luo, J.-J., S. Masson, S. K. Behera, et al., 2008: Extended ENSO predictions using a fully coupled
 493 ocean–atmosphere model. *J. Clim.*, **21**, 84–93, doi: 10.1175/2007JCLI1412.1.
- 494 Saha, S., S. Moorthi, H. L. Pan, et al., 2010: The NCEP climate forecast system reanalysis. *Bull. Am.*
 495 *Meteor. Soc.*, **91**, 1015–1057, doi: 10.1175/2010BAMS3001.1.

- 496 Singleton, T., 2011: Data assimilation experiments with a simple coupled ocean- atmosphere model.
 497 Ph. D. dissertation, University of Maryland, College Park, 116 pp.
- 498 Sugiura, N., T. Awaji, S. Masuda, et al., 2008: Development of a four-dimensional variational coupled
 499 data assimilation system for enhanced analysis and prediction of seasonal to interannual climate
 500 variations. *J. Geophys. Res. Ocean.*, **113**(C10), C10017, doi: 10.1029/2008JC004741.
- 501 Tardif, R., G. J. Hakim, and C. Snyder, 2015: Coupled atmosphere–ocean data assimilation
 502 experiments with a low-order model and CMIP5 model data. *Climate Dyn.*, **45**, 1415–1427, doi:
 503 10.1007/s00382-014-2390-3.
- 504 Uppala, S. M., P. W. Kållberg, A. J. Simmons, et al., 2005: The ERA-40 re-analysis. *Quart. J. Roy.
 505 Meteor. Soc.*, **131**, 2961–3012, doi: 10.1256/qj.04.176.
- 506 Zhang, S., 2011: A study of impacts of coupled model initial shocks and state-parameter optimization
 507 on climate predictions using a simple pycnocline prediction model. *J. Clim.*, **24**, 6210–6226, doi:
 508 10.1175/JCLI-D-10-05003.1.
- 509 Zhang, F., C. Snyder, and J. Z. Sun, 2004: Impacts of initial estimate and observation availability on
 510 convective-scale data assimilation with an ensemble Kalman filter. *Mon. Wea. Rev.*, **132**, 1238–1253,
 511 doi: 10.1175/1520-0493(2004)132<1238:IOIEAO>2.0.CO;2.
- 512 Zhang, S., M. J. Harrison, A. T. Wittenberg, et al., 2005: Initialization of an ENSO forecast system
 513 using a parallelized ensemble filter. *Mon. Wea. Rev.*, **133**, 3176–3201, doi: 10.1175/MWR3024.1.
- 514 Zhang, S., M. J. Harrison, A. Rosati, et al., 2007: System design and evaluation of coupled ensemble
 515 data assimilation for global oceanic climate studies. *Mon. Wea. Rev.*, **135**, 3541–3564, doi:
 516 10.1175/MWR3466.1.
- 517
- 518